

# Magnetic structure of $\text{MgCu}_2\text{O}_3$ and doping-induced spin reorientation in $\text{Mg}_{1-x/2}\text{Li}_x\text{Cu}_{2-x/2}\text{O}_3$

M. Winkelmann and H. A. Graf

*Hahn-Meitner-Institut, Glienicker Strasse 100, D-14109 Berlin, Federal Republic of Germany*

N. H. Andersen

*Risø National Laboratory, DK-4000 Roskilde, Denmark*

(Received 14 June 1993)

The magnetic properties of undoped and Li-doped  $\text{MgCu}_2\text{O}_3$  single crystals have been studied by magnetic-susceptibility and neutron-diffraction measurements. The pure compound is a semiconductor with an antiferromagnetic ground state ( $T_N=95$  K). Above  $T_N$ , short-range magnetic correlations within the Cu-O chains of the  $\text{MgCu}_2\text{O}_3$  structure give rise to a predominantly one-dimensional (1D) magnetic behavior. This is revealed by the quantitative interpretation of the susceptibility measurements. Below  $T_N$ , the 3D magnetic structure, derived from neutron-diffraction experiments, can be described by an essentially collinear model. A small spin canting, however, exists, because adjacent  $\text{CuO}_6$  octahedra are strongly tilted with respect to each other. The magnetic structure can be decomposed into two independent magnetic sublattices, which, in the mean-field approximation, are not coupled. The topology is similar to the one producing an infinitely degenerate state in antiferromagnetic fcc lattices. Doping experiments with Li clearly demonstrate the importance of spin fluctuations and fluctuations of the local exchange fields for lifting the degeneracy in such a system. A remarkably small amount of Li (about 2 mole % Li) is sufficient to disturb the magnetic lattice in such a way that the almost collinear spin arrangement changes into an arrangement where the spins of one sublattice are strongly canted with respect to the spins of the other sublattice.

## INTRODUCTION

An interesting feature of the high- $T_c$  superconducting CuO systems is the strong magnetic interaction between the Cu spins. Since the discovery of high- $T_c$  superconductivity,<sup>1</sup> many studies have been performed with the objective of understanding the relationship between magnetism and superconductivity in these systems.<sup>2-6</sup>

The present study is concerned with the magnetic properties of a simple ternary Cu-O system,  $\text{MgCu}_2\text{O}_3$ , which is a semiconductor with  $E_g \approx 0.94$  eV. The doping with Li leads to a strong increase of the electrical conductivity, which can be described by the Mott variable-range-hopping law.<sup>7,8</sup> No metallic conductivity or superconductivity is observed. The chemical structure (space group Pmmn;  $a=3.99$  Å,  $b=9.33$  Å,  $c=3.18$  Å) of  $\text{MgCu}_2\text{O}_3$  was determined by Drenkhahn and Müller-Buschbaum.<sup>9</sup> Figure 1 shows the fourfold chemical unit cell (the  $a$  and  $b$  axes are doubled) of  $\text{MgCu}_2\text{O}_3$ . The Cu atoms are connected by  $180^\circ$  Cu—O—Cu bonds to form Cu-O chains parallel to the  $a$  axis. In planes perpendicular to the  $a$  axis, the Cu-atoms are linked by approximately  $90^\circ$  Cu—O—Cu bonds. The local coordination of each Cu atom is a strongly elongated O octahedron with four short equatorial bonds (bondlengths 1.93–2.0 Å) and two long axial bonds (bondlengths 2.54 and 2.77 Å) (Fig. 2). Two neighboring Cu-O chains are linked via common O-O edges of the equatorial planes of the  $\text{CuO}_6$  octahedra to form Cu-O ribbons. These ribbons are connected by approximately  $90^\circ$  Cu—O—Cu and O—Mg—O bonds to form corrugated two-dimensional structural entities

parallel to  $a$  and  $b$ . In three dimensions these entities are interconnected only via the Mg-O (bondlength 2.6 Å) and the long axial Cu-O bonds. A section of such a quasi-layer is shown in Fig. 2. It can be seen that the long axes of the  $\text{CuO}_6$  octahedra in neighboring ribbons are oppositely rotated around the  $a$  axis to include an angle  $\alpha = \pm 38^\circ$  with the  $c$  axis.

Neutron diffraction and susceptibility measurements of  $\text{MgCu}_2\text{O}_3$  were performed on powder samples by Zeiske, Graf, and Dachs.<sup>10</sup> The authors reported an onset of 3d

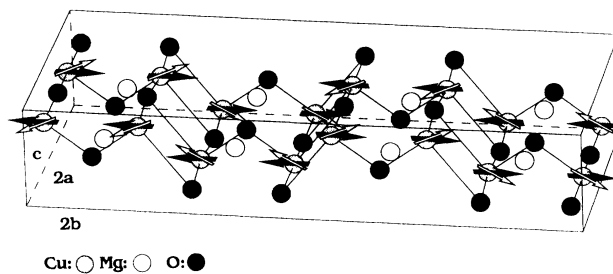


FIG. 1. The magnetic unit cell of  $\text{MgCu}_2\text{O}_3$ . The  $a$  and  $b$  axes are doubled as compared to the chemical unit cell. All spins in the upper part of the unit cell belong to the one magnetic sublattice, all spins in the lower part belong to the other sublattice. The spin arrangement for the undoped system is symbolized by the black arrows. In slightly Li-doped samples an additional phase transition occurs, where the spins of both sublattices are strongly rotated in opposite direction, giving rise to a large canting angle between the two sublattices. This is shown by the white arrows.

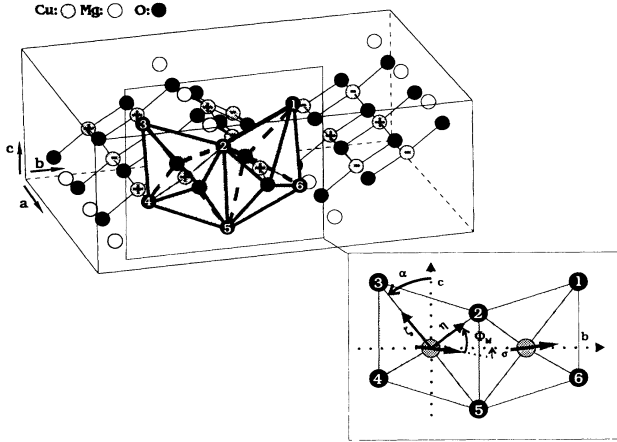


FIG. 2. The equatorial planes of the  $\text{CuO}_6$  octahedra are linked via common edges to form ribbons parallel to  $a$ . These ribbons are connected by approximately  $90^\circ$   $\text{O—Mg—O}$  and  $\text{Cu—O—Cu}$  bonds to a corrugated quasiplane. Adjacent  $\text{CuO}_6$  octahedra are tilted in opposite direction, giving rise to a weak spin canting in the undoped and doped system. This spin canting is shown in more detail in the inset.

antiferromagnetic order at  $T_N = 95$  K. Experiments performed during the present study showed that doping with Li decreases the Néel temperature drastically.<sup>7</sup> To determine the magnetic structure in more detail than was possible in the former study on powder samples and to investigate the influence of Li doping, we have performed susceptibility measurements and neutron-diffraction measurements on pure and Li doped  $\text{MgCu}_2\text{O}_3$ , mainly using single crystals as samples.

## I. EXPERIMENT

### A. Sample preparation and characterization

The single crystals of  $\text{MgCu}_2\text{O}_3$  were grown from a KF flux by slow cooling. A mixture of KF, polycrystalline  $\text{MgCu}_2\text{O}_3$  and an additional amount of MgO were heated up in a platinum crucible to 1310 K. In the case of doped crystals, Li-doped polycrystalline  $\text{MgCu}_2\text{O}_3$  and an additional amount of  $\text{Li}_2\text{O}$  were used as starting material. After 12 h for homogenization, the mixture was cooled down with a slow rate of 1 K/h. By this method needle-like single crystals with dimensions up to  $7 \times 2 \times 0.3$  nm<sup>3</sup> and a good crystallographic quality were obtained. The Li concentrations of the doped crystals were determined by chemical analysis to be about 3 mole %. It was not possible to grow single crystals with a higher Li content, whereas single-phase powder samples with a Li concentration up to 12 mole % could be prepared.

To obtain single-phase powder samples of pure and Li doped  $\text{MgCu}_2\text{O}_3$ , however, an excess of Cu (about 10 mole %) in the starting material was necessary. Neutron-powder-diffraction measurements and x-ray studies on single crystals established that the system is inevitably structurally disordered: in the powder samples as well as in the single crystals part of the Mg site (10–20 %) is always occupied by Cu atoms. The partial substitu-

tion of Mg by Cu seems to stabilize the  $\text{MgCu}_2\text{O}_3$  structure. This observation is highly surprising, since the  $\text{Mg}^{2+}$  ion is located at the center of a compressed O octahedron ( $\text{Mg—O}$  bonds  $4 \times 2.16$  and  $2 \times 2.01$  Å). Such a coordination is very unusual for the Jahn-Teller ion  $\text{Cu}^{2+}$ , which normal favors an elongated octahedron. Up to now, compressed  $\text{CuO}_6$  octahedra were only observed in a few mixed systems,<sup>11</sup> in which the local environment is imposed by the host lattice. A detailed discussion of this interesting structural aspect will be given elsewhere.<sup>12</sup>

### B. Magnetic susceptibility measurements

The magnetic susceptibility of undoped and slightly Li-doped  $\text{MgCu}_2\text{O}_3$  was measured by a superconducting quantum interference device (SQUID)–magnetometer on small single crystals (3–5 mg) between 2 and 360 K. Because of the small sample volumes a relatively high magnetic field of  $B = 1$  T was applied to obtain a good resolution.

The magnetic susceptibilities of  $\text{MgCu}_2\text{O}_3$  with  $B \parallel a$ ,  $B \parallel b$ , and  $B \parallel c$  are shown in Fig. 3(a). The onset of the  $3d$  magnetic order at  $T_N = 96 \pm 1$  K can clearly be seen for  $B \parallel b$ . The susceptibility for  $B \parallel a$  and  $B \parallel c$  continues to increase with decreasing temperature. It can be concluded, that the major spin direction of the ordered state should be parallel to the  $b$  axis, which is conformed with the neutron measurements discussed later. Normally, the antiferromagnetic susceptibility  $\chi_{\parallel}$  should decrease to zero when lowering the temperature, which is not observed in the present case. This unusual feature is discussed below.

The Néel temperature reacts very sensitively to doping with Li. This was demonstrated by doping experiments on powder samples.<sup>7</sup> The critical concentration, above which a long-range magnetic order cannot be observed any longer, is about 13 mole % Li. From Rietveld refinements of neutron powder measurements performed on doped samples, it can be concluded that approximate-

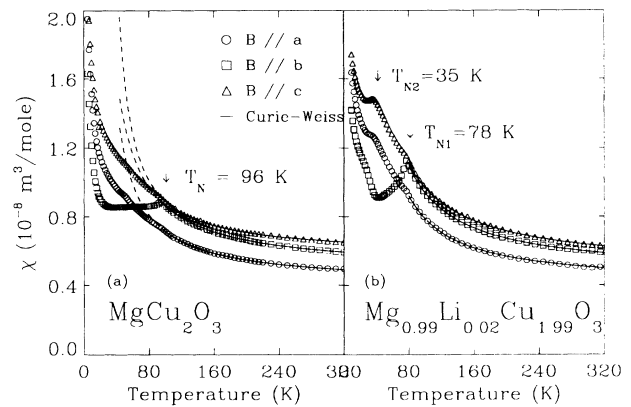


FIG. 3. The magnetic susceptibility of undoped (a) and slightly Li-doped (b)  $\text{MgCu}_2\text{O}_3$  vs the temperature. The data above  $T_N$  can very well be fitted by a Curie-Weiss law plus a large constant contribution [ $\chi = \chi_0 + C/(T - \Theta)$ ]. These fits are represented by the solid curves. The dashed curves in (a) show the continuation of these fits for  $T < T_N$ .

ly one half of the Li ions are located at the Cu positions. The stoichiometric composition of the doped samples can be expressed as  $\text{Mg}_{1-x/2}\text{Li}_x\text{Cu}_{2-x/2}\text{O}_3$ .<sup>7</sup> In addition to a simple depression of the magnetic order with increasing Li contribution, a spin reorientation at low temperature occurs, which is clearly visible in neutron diffraction and susceptibility measurements performed on single crystals. Figure 3(b) shows the  $\chi(T)$  data for a slightly doped crystal ( $x=0.02$ ). The small amount of Li is sufficient to change the magnetic susceptibility below  $T_N$ . At  $T_{N2}=35$  K an anomaly appears, which indicates a transition to a new magnetic order.

### C. Neutron-diffraction measurements

The measurement on the undoped single crystal (volume =  $7 \times 2 \times 0.3$  mm<sup>3</sup>) were performed on the triple axis spectrometer E1 at the Hahn-Meitner Institut in Berlin, and the measurement on the doped single crystal (the volume is  $7 \times 1 \times 0.3$  mm<sup>3</sup>) on the triple axis spectrometer TAS1 at the Risø National Laboratory. Because of the small crystal size and the low magnetic moment of  $\text{Cu}^{2+}$  the signal to noise ratio had to be optimized carefully. In both cases the samples were measured in the elastic mode of the triple axis spectrometers using a coarse collimation. The wavelength used was 2.4 Å and the monochromator and analyzer crystals were pyrolytic graphite (PG). A PG filter was used for suppressing higher-order-wavelength contaminations. The samples were cooled in closed-cycle displax He cryostats.

In the investigated undoped crystal the onset of the magnetic order occurs at  $T_N=95 \pm 1$  K. A series of magnetic Bragg reflections were measured at the lowest possible temperature (8.5 K). In a second experiment the dataset was completed by measuring the two very weak reflections  $(1/2, 3/2, 0)$  and  $(3/2, 3/2, 0)$ . To increase the diffracting volume in this case, three crystals were mounted on a special sample holder, which allowed a pre-

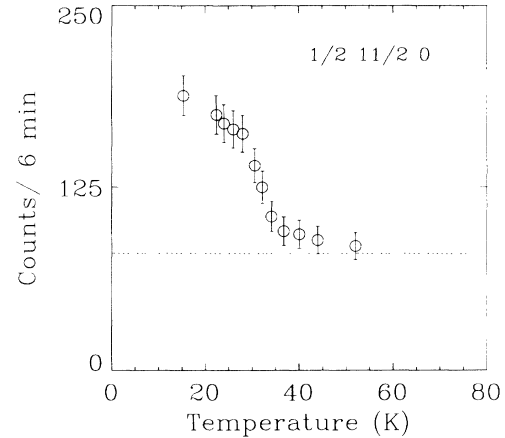


FIG. 4. The neutron peak intensity at the position  $(1/2, 11/2, 0)$  vs the temperature. Above  $T_{N2}=35 \pm 1$  K a magnetic reflection cannot be observed (the dotted line represents the background). Below this temperature the onset of the spin canting between both magnetic sublattices leads to a strong increase of the diffracted intensity.

cise mutual orientation of three crystals. The integrated intensities of the observed reflections are listed in Table I. The magnetic superstructure reflections are commensurate and indicate a magnetic unit cell, where the  $a$  and  $b$  axes of the chemical unit cell are doubled, but not the  $c$  axis.

The susceptibility measurements on slightly doped single crystals point to a second magnetic phase transition at  $T_{N2}=35 \pm 1$  K. To study the changes in the magnetic structure of Li-doped  $\text{MgCu}_2\text{O}_3$ , neutron-diffraction experiments were performed on TAS1 in Risø on a single crystal with the composition  $\text{Mg}_{0.99}\text{Li}_{0.02}\text{Cu}_{1.99}\text{O}_3$ . A series of magnetic reflections was measured at  $T=16$  K ( $T < T_{N2}$ ) and at  $T=52$  K ( $T_{N2} < T < T_{N1}$ ). The data are

TABLE I. Comparison between observed and calculated intensities for the undoped single crystal  $\text{MgCu}_2\text{O}_3$  at  $T=8.5$  K ( $\mu_{\text{ord}}=0.32 \pm 0.02 \mu_B$ ). The small but significant intensities found for the reflections  $(1/2, 3/2, 0)$  and  $(3/2, 3/2, 0)$  indicate a slight spin canting of  $\sigma=7 \pm 1^\circ$  [angle between the direction of the magnetic moment and the  $b$  axis within the  $(100)$  plane]. The indices refer to the chemical unit cell.

H	K	L	$I(\text{obs})$	$I(\text{calc})$		
				$\sigma=7^\circ$	$\sigma=0^\circ$	
1/2	1/2	0	487.0±21.0	426.2	430.2	
1/2	3/2	0	6.2±1.8	6.3	0.12	
1/2	5/2	0	31.3±4.3	32.9	32.3	
1/2	7/2	0	14.0±3.5	13.1	12.8	
3/2	1/2	0	153.0±9.5	125.5	126.8	
3/2	3/2	0	2.7±0.8	2.3	0.09	
3/2	5/2	0	47.0±4.6	55.9	56.2	
3/2	7/2	0	25.5±3.1	36.1	36.4	
1/2	1/2	1	131.5±8.5	147.6	149.7	
1/2	5/2	1	65.0±7.5	58.5	59.2	
1/2	7/2	1	31.8±6.0	35.7	36.1	
				$R_m = 100(\sum w[I(\text{obs}) - I(\text{calc})]^2 / [\sum wI(\text{obs})^2])^{1/2}$	16.2	21.7
				$GOF_M = 100(\sum w[I(\text{obs}) - I(\text{calc})]^2 / (N_0 - N_p))^{1/2}$	2.3	3.08

TABLE II. Comparison between observed and calculated intensities for the slightly Li-doped single crystal  $\text{Mg}_{0.99}\text{Li}_{0.02}\text{Cu}_{1.99}\text{O}_3$  at  $T=52$  K ( $T_{N2} < T < T_{N1}$ ) and at  $T=16$  K ( $T < T_{N2}$ ). The data are scaled by the averaged ratio of the nuclear intensities of the undoped crystal to the nuclear intensities of the doped crystal to be the same scale as the data in Table I. The data of Tables I and II are, therefore, comparable. The magnetic structure above  $T_{N2}$  is identical to the magnetic structure of the undoped system. Below  $T_{N2}$  the spin directions of both sublattices enclose an angle  $\pm\gamma$  with the  $b$  axis (canting angle =  $2\gamma$ ). The integrated intensities calculated for two models are given: a spin turn in the (100) plane ( $\gamma_a$ ) and a spin turn in the (001) plane ( $\gamma_c$ ). The magnetic moment was determined to be  $\mu_{\text{ord}} = 0.32 \pm 0.02 \mu_B$ .

H	K	L	$T=52$ K		$T=16$ K		
			$I$ (obs)	$I$ (calc)	$I$ (obs)	$I$ (calc)	$\gamma_a=32^\circ$
1/2	1/2	0	278.2±12.3	242.6	381.1±11.8	342.8	323.5
-1/2	1/2	0	240.6±11.2	242.6	345.3±13.5	342.8	323.5
1/2	5/2	0	14.9±4.6	18.8	56.4±4.0	56.2	58.5
-1/2	5/2	0		18.8	59.2±5.3	56.2	58.5
1/2	7/2	0	4.1±2.1	7.5	36.7±3.7	34.1	36.5
1/2	7/2	0	4.9±3.7	7.5	45.1±5.0	34.1	36.5
1/2	11/2	0	0.7±1.8	1.3	18.9±3.8	10.9	12.0
3/2	1/2	0	66.9±6.7	71.5	95.8±6.9	96.6	90.4
3/2	5/2	0	21.8±4.4	31.8	34.3±4.0	48.8	46.8
-3/2	5/2	0		31.8	29.6±4.1	48.8	46.8
3/2	7/2	0	12.2±3.4	20.6	25.3±3.7	35.4	34.5
1/2	-1/2	-1	75.0±10.3	83.8	79.6±9.5	86.6	137.2
$R_M$				14.3		15.4	19.7
$GOF_M$				3.0		3.5	4.1

listed in Table II. At low temperature the intensities of magnetic reflections with large  $k$  indices are strongly increased in comparison with the measurement at  $T=52$  K. The intensity versus temperature scans of the magnetic reflections [e.g., the (1/2, 11/2, 0) reflection in Fig. 4] show that the intensity starts to increase at  $T_{N2}=35$  K, where the second anomaly had been found in the magnetic susceptibility of the doped crystal.

## II. DISCUSSION

### A. The magnetic susceptibility of undoped and Li-doped $\text{MgCu}_2\text{O}_3$

The magnetic susceptibility of undoped and Li-doped  $\text{MgCu}_2\text{O}_3$  is different only below  $T_N$ , where a second magnetic phase transition occurs in the doped crystals. The spin arrangement of this new magnetic phase will be discussed in Sec. II C. Above the Néel temperature the  $\chi(T)$  curves in Figs. 3(a) and 3(b) can very well be fitted by a Curie-Weiss law plus a large constant term. The effective paramagnetic moment  $\mu_{\text{eff}} = g\mu_B [S(S+1)]^{1/2}$  is determined in both cases to be  $0.30 \pm 0.03 \mu_B$ . This is much less than the theoretical prediction of  $1.73 \mu_B$  for a spin- $\frac{1}{2}$  system. The magnetic susceptibility can consistently be explained by assuming a nearly  $1d$  antiferromagnetic behavior above  $T_N$ . This assumption is plausible considering the Cu-O chains in the structure with  $180^\circ$  Cu—O bonds. As predicted by the Goodenough-Kanamori rules<sup>13,14</sup> the  $180^\circ$  Cu—O—Cu bond along the chains allows a strong antiferromagnetic coupling of the spins, whereas the approximately  $90^\circ$  Cu—O—Cu bond

between the chains should only lead to weak ferromagnetic interactions. The  $180^\circ$  Cu—O bondlength in  $\text{MgCu}_2\text{O}_3$  (2.00 Å) is slightly larger than the corresponding value in  $\text{La}_2\text{CuO}_4$  (1.91 Å).<sup>15</sup> Using the power law  $|J| \propto (\text{bondlength})^{-n}$  with  $n \approx 11, \dots, 12$  (Ref. 16) and the value  $|J|/k_B = 1300$  K for  $\text{La}_2\text{CuO}_4$  (Ref. 17) an intra-chain coupling constant of about  $|J|/k_B \approx 770$  K can be estimated for  $\text{MgCu}_2\text{O}_3$ .

The typical susceptibility of  $1d$   $S = \frac{1}{2}$  system has a very broad maximum around the characteristic temperature  $T_{1d}^* \approx 1.28|J|/k_B$  and a constant value for  $T \rightarrow 0$ .<sup>18</sup> The observed paramagnetic increase of  $\chi(T)$  with decreasing temperature can be explained by the presence of 3.5 mole %  $\text{Cu}^{2+}$  ions with a full paramagnetic spin- $\frac{1}{2}$  moment. Since the  $\text{MgCu}_2\text{O}_3$  structure is intrinsically disordered, as was discussed before, a certain amount of  $\text{Cu}^{2+}$  ions is inevitably occupying Mg sites. These may only be weakly coupled to the regular magnetic structure and could, thus, act as paramagnetic impurities. Paramagnetic behavior may also be caused by finite-size chain effects, if the magnetic system does not consist of ideally  $1d$  infinite chains.<sup>18</sup> We conjecture, that both effects, finite chains and  $\text{Cu}^{2+}$  ions on the Mg site, combine to give the observed Curie-Weiss-type contribution to the susceptibility above  $T_N$ . Below  $T_N$  the paramagnetism from both these defects compensates the otherwise expected decrease of  $\chi(B||b)$  and masks the constant intrinsic susceptibility  $\chi(B||a)$  and  $\chi(B||c)$ .

Before comparing the constant term fitted to the measured susceptibility with the value expected for a quasi-uniform  $1d$  susceptibility below room temperature one

has to correct for the diamagnetic and the Van Vleck susceptibility, which also give constant contributions:

$$\chi_{\alpha\alpha} = \chi_{\alpha\alpha}^{1d} + \chi_{\alpha\alpha}^{\text{dia}} + \chi_{\alpha\alpha}^{\text{VV}} \quad (\alpha = x, y, z). \quad (1)$$

The value for the diamagnetic susceptibility can be calculated from the single ion diamagnetism to be  $-0.08 \text{ m}^3/\text{mole}$ .<sup>19</sup> The expression for the Van Vleck susceptibility can be written as:<sup>20</sup>

$$\chi_{\alpha\alpha}^{\text{VV}} = 2 \frac{N}{V} \mu_0 \mu_B^2 \sum_n \frac{|\langle n | L_\alpha | \Psi_g \rangle|^2}{E_n - E_0} = 2 \frac{N}{V} \mu_0 \mu_B^2 \Lambda_{\alpha\alpha}. \quad (2)$$

$N/V$ ,  $\mu_0$ , and  $L_\alpha$  denote the number of spins per volume, the permeability, and the component of the orbital angular momentum,  $|\Psi_g\rangle$  represents the electronic ground state with the energy  $E_0$ , and  $|n\rangle$  are excited states of energy  $E_n$ . The wave function of the singly occupied  $d$  orbital of a  $\text{Cu}^{2+}$  ion in a Jahn-Teller distorted environment is given by<sup>21</sup>

$$|\Psi_g\rangle = \sin \frac{\phi}{2} |d_{3\xi^2-r^2}\rangle + \cos \frac{\phi}{2} |d_{\xi^2-\eta^2}\rangle$$

with (3)

$$\tan \phi = \sqrt{3} \frac{d_\xi - d_\eta}{2d_\xi - d_\xi - d_\eta}.$$

$\xi$ ,  $\eta$ , and  $\zeta$  are the principal axes of the  $\text{CuO}_6$  octahedra ( $\zeta$  is parallel to the long axis, and  $\xi$  and  $\eta$  lie in the equatorial plane of the distorted octahedron). Using Eq. (3) with the experimentally determined Cu—O bond lengths  $d_\xi = 2.00 \text{ \AA}$ ,  $d_\eta = 1.93 \text{ \AA}$ , and  $d_\zeta = 2.65 \text{ \AA}$ , the matrix elements of the Van Vleck susceptibility can be evaluated. For finally calculating the Van Vleck susceptibility, a uniform value of  $9000 \text{ cm}^{-1}$  for the energy separation  $E_n - E_0$  due to the crystal field and a covalency factor of  $k_{\text{cov}} = 0.8$  correcting for covalency effects in the Cu—O bonds have been assumed. Both values are typical for  $\text{Cu}^{2+}$  ions in Jahn-Teller distorted octahedral environments.<sup>21</sup>

The magnetic susceptibility for a  $1d$  antiferromagnetic isotropic Heisenberg system was theoretically derived by Bonner and Fisher.<sup>18</sup> For a very large coupling constant ( $|J|/k_B \gg 300 \text{ K}$ ) the susceptibility below room temperature can be approximated by a uniform value. Using Ref. 18 and assuming  $|J|/k_B \approx 770 \text{ K}$ , the following contribution to the susceptibility of  $\text{MgCu}_2\text{O}_3$  can be estimated:

$$\begin{aligned} \chi_{\alpha\alpha}^{1d}(\text{MgCu}_2\text{O}_3, T < 300\text{K}) \\ \approx \chi_{\alpha\alpha}^{1d}(\text{MgCu}_2\text{O}_3, T = 300\text{K}) \\ \approx 6.95 \times 10^{-10} g_{\alpha\alpha}^2 \text{ m}^3/\text{mole}. \end{aligned} \quad (4)$$

$g_{\alpha\alpha}$  denotes the gyromagnetic ratio. The  $g$  factors can be calculated from the relation  $g_{\alpha\alpha} = 2(1 - \lambda k_{\text{cov}}^2 \lambda_{\alpha\alpha})$ . Taking the free ion LS coupling of  $\lambda = -830 \text{ cm}^{-1}$ ,<sup>22</sup> the following values are derived:  $g_{xx} = 2.14$ ,  $g_{yy} = 2.25$ , and  $g_{zz} = 2.34$ . Using these  $g$  values,  $1d$  magnetic susceptibilities are calculated, which are in a good agreement with the values obtained by subtracting the diamagnetic and

TABLE III. The different contributions to the quasi constant term  $\chi_0$  of the magnetic susceptibility of  $\text{MgCu}_2\text{O}_3$  ( $T > T_N$ ). For details see text.

( $\times 10^{-8} \text{ m}^3/\text{mole}$ )	$B  a$	$B  b$	$B  c$
$\chi^{\text{dia}}$ (calc)	-0.08	-0.08	-0.08
$\chi^{\text{VV}}$ (calc)	$0.11 \pm 0.02$	$0.19 \pm 0.03$	$0.26 \pm 0.03$
$\chi^{1d}$ (calc)	$0.32 \pm 0.03$	$0.35 \pm 0.03$	$0.38 \pm 0.03$
$\chi^{1d}$ (expt) $\equiv \chi_0^{\text{nt}} - \chi^{\text{dia}} - \chi^{\text{VV}}$	$0.38 \pm 0.03$	$0.37 \pm 0.03$	$0.40 \pm 0.03$

Van Vleck susceptibilities from the measured constant contribution. The values are listed in Table III.

### B. The magnetic structure of undoped $\text{MgCu}_2\text{O}_3$

The model of the magnetic structure shown in Fig. 1 (black arrows) was derived by applying the Goodenough-Kanamori exchange rules<sup>13,14</sup> (antiferromagnetic coupling along the  $180^\circ$  and ferromagnetic coupling along the  $90^\circ$  Cu—O—Cu bond). The intensities calculated for this model are in good agreement with the measured data, if one assumes that the spin direction is parallel to the  $b$  axis (Table I). For all calculations the isotropic approximation of the ionic  $\text{Cu}^{2+}$  form factor was used.<sup>23</sup> Major discrepancies exist only for the reflections  $(1/2, 3/2, 0)$  and  $(3/2, 3/2, 0)$ , which should be almost extinguished for the collinear model, whereas small intensities have been found in the experiment.

These deviations point to a slight spin canting, which can be understood as a result of the large tilt angle between the long axes of adjacent  $\text{CuO}_6$  octahedra. Various reasons for the occurrence of a spin canting are discussed in literature.<sup>24</sup> In the  $\text{MgCu}_2\text{O}_3$  system two mechanisms have to be regarded: the antisymmetric exchange coupling<sup>25</sup> (Dzialoshinski-Moriya interaction) and the interaction of differently oriented anisotropic  $g$  tensors.<sup>26</sup>

Symmetry restrictions determine the orientation of the Dzialoshinski-Moriya interaction vector  $D$ .<sup>25</sup> The Cu positions with oppositely rotated  $\text{CuO}_6$  octahedra are not related by an inversion symmetry but by a mirror plane parallel to  $(010)$  and a twofold rotation axis parallel to  $c$ . It follows that  $D$  must lie in direction of the  $a$  axis, and the ground-state energy is minimized by a spin canting in the  $(100)$  plane. The resulting canting angle  $\sigma$  between the spin direction and the  $b$  axis can be estimated from the expression  $\tan \sigma \sim (g - 2)/g$  (Ref. 25) to be  $\sigma \approx 3.7^\circ$  using  $g_x = g_\xi = 2.14$ .

Silvera, Thornley, and Tinkham<sup>26</sup> show that a strong spin canting can also occur by an interaction between two spins with differently oriented anisotropic  $g$  tensors. If the two  $g$  tensors are oppositely rotated by an angle  $\alpha$  around an axis parallel to the  $a$  axis, the canting angle can be calculated by the relations:

$$\tan \phi_M = \frac{g_\xi}{g_\eta} \tan \phi_s$$

with

$$\tan 2\phi_s = - \frac{2g_\eta g_\xi \tan 2\alpha}{(g_\eta)^2 + (g_\xi)^2}. \quad (5)$$

The principle axes  $g_\xi$ ,  $g_\eta$ ,  $g_\zeta$  of the  $g$  tensor are oriented parallel to the local axes of the  $\text{CuO}_6$  octahedra.  $\Phi_M$  denotes the angle between the  $\eta$  axis and the magnetic moment (see Fig. 2). With the estimated  $g$  values of  $\text{MgCu}_2\text{O}_3$  ( $g_\xi \approx 2.14$ ,  $g_\eta \approx 2.10$ ,  $g_\zeta \approx 2.47$ ) and  $\alpha = 38^\circ$  a canting angle of  $|\sigma| = |\alpha - \Phi_M| \approx 4.5^\circ$  can be calculated from Eqs. (5).

Both mechanisms, thus, give rise to a small spin component parallel to the  $c$  axis in  $\text{MgCu}_2\text{O}_3$ . These  $c$  components form an antiferromagnetic array with a configurational symmetry different from that of the basic magnetic structure spanned by the major spin components (see inset of Fig. 2). The two strongest reflections of a magnetic structure formed only by the  $c$  components would be  $(1/2, 3/2, 0)$  and  $(3/2, 3/2, 0)$ , whereas these are almost extinguished in the basic collinear model. Observing these reflections is very indicative, therefore, that the predicted spin canting exists. The best fit to the data is achieved for an angle  $\sigma = 7 \pm 1^\circ$  (Table I), which has the same order of magnitude as the values estimated by the two mechanisms discussed.

The ordered magnetic moment was determined to be  $\mu_{\text{ord}} = 0.32 \pm 0.02 \mu_B$  by scaling the intensity of the magnetic reflections with the intensity of the nuclear reflections. This value is much less than the  $1.1 \mu_B$  ( $g_{yy} \approx 2.25$ ) expected for a completely ordered  $S = \frac{1}{2}$  Néel state. Zero-point quantum fluctuations and covalency effects can lead to a reduction of the ordered magnetic moment.<sup>27</sup> The theoretical calculation for the reduction due to quantum fluctuations can be performed applying the linear-spin-wave theory. In the special case of low dimensional  $S = 1/2$  systems an additional kinematical correction is necessary.<sup>28,29</sup> Simplifying the structure of  $\text{MgCu}_2\text{O}_3$  as a quadratic arrangement of antiferromagnetic chains, the Néel temperature is given by  $T_N \approx 2.07 \times S(S+1) |JJ'|^{1/2}$  and the ratio  $|J/J'| \approx 160$  can be estimated.<sup>30</sup> This leads to a quantum reduction of  $\Delta S_{zpf} = 0.26$  and to an ordered magnetic moment of  $\mu_{\text{ord, reduced}} = 0.54 \mu_B$  for the simplified  $\text{MgCu}_2\text{O}_3$  structure. A further reduction of about 20%—possibly due to covalency effects<sup>27</sup>—is necessary to obtain the measured value.

### C. The magnetic structure of Li-doped $\text{MgCu}_2\text{O}_3$

At  $T = 52$  K the neutron measurements on the Li-doped single-crystal  $\text{Mg}_{0.99}\text{Li}_{0.02}\text{Cu}_{1.99}\text{O}_3$  are in good agreement with the nearly collinear magnetic model derived for the undoped system (see Table II). Below  $T_{N2} = 35$  K; however, a strong increase of the intensity for magnetic reflections with large  $k$  indices occurs. This can be explained by the formation of a new magnetic structure, where the spins of the two magnetic sublattices are rotated by a large angle either in the same direction or in opposite directions. When averaging over the possible magnetic domains, both spin configurations give the same intensity distribution. It will be discussed in the following, however, that the magnetic structure is correctly described by that configuration, where the spins of one sublattice are oppositely rotated to the spins of the other

sublattice.

The spin reorientation leading to the new magnetic phase can be understood on the basis of a general principle: “ordering due to disorder”.<sup>31–33</sup> Many highly symmetric spin systems with competing exchange interactions have a degenerate magnetic ground state. These systems can be divided into different antiferromagnetic subsystems, which, in the mean-field approximation, are not coupled to each other. In the case of  $\text{MgCu}_2\text{O}_3$  one finds two independent subsystems (e.g., the four upper Cu atoms in Fig. 1 belong to the one and the four lower Cu atoms to the other subsystem). The degeneracy arises because the local exchange fields induced by the spins of the one subsystem just cancel at the spin positions of the other subsystem. In absence of any anisotropy, the relative orientation of the spin direction between the two subsystems is not fixed. Recent theories predict that this degeneracy is lifted by spin fluctuations, like thermal and quantum fluctuations, and by fluctuations of the local exchange field because of nonmagnetic impurities.<sup>31–33</sup> The detailed theoretical discussion shows, that thermal spin fluctuations and quantum fluctuations favor a collinear spin arrangement of both magnetic sublattices and the fluctuations of the local exchange field, e.g., by diluting the magnetic system with unmagnetic ions, favor an anticolinear arrangement (i.e., canting angle  $2\gamma = 90^\circ$ ). The canting in such a dilute magnetic system is not only a local effect in the environment of the unmagnetic impurity. It must be regarded as a new ground state of the whole system.

In general, Cu-O systems exhibit only a weak anisotropy because of the absence of the single-ion anisotropy in a spin- $\frac{1}{2}$  system. The spin direction is mainly fixed by the weak dipole-dipole interaction and the anisotropic exchange interaction. For such systems with weak anisotropy the effects of spin or exchange field fluctuations are very important for the magnetic ground state. This is demonstrated by doping the system  $\text{MgCu}_2\text{O}_3$  with unmagnetic  $\text{Li}^+$  ions. At higher temperature a collinear arrangement of the spins is stabilized by thermal spin fluctuations (like in the undoped system). When lowering the temperature the magnitude of the thermal spin fluctuations decreases. At  $T_{N2} = 35$  K the fluctuations of the exchange field due to the unmagnetic dilution of the magnetic lattice compensate the stabilizing effect of the thermal fluctuations, and below this temperature the new ground state is a strongly canted spin arrangement of both magnetic sublattices.

The best agreement between  $I(\text{obs})$  and  $I(\text{calc})$  was obtained for a canting angle of  $\gamma \approx \pm 30^\circ$  between the  $b$  axis and the spin direction. The magnetic moment was determined to be  $\mu_{\text{ord}} = 0.32 \pm 0.02 \mu_B$ , and, thus, has the same value as in the undoped crystal. The data measured at 16 K are compatible with two models, one where the spins are rotated in the (001) plane and another, where the spins are rotated in the (100) plane. A comparison between the experimental intensities and the intensities calculated for these two models is given in Table II, where the angle between the spin direction and the  $b$  axis is denoted by  $\gamma_c$  and  $\gamma_a$ , respectively, for the two cases. The model describing a spin rotation in the (100) plane

( $\gamma_a$ ) is slightly favored by a somewhat better fit and  $R$  value.

### CONCLUSIONS

$\text{MgCu}_2\text{O}_3$  is a weakly canted antiferromagnet with a Néel temperature of 95 K. The magnetic structure is consistent with the Goodenough-Kanamori superexchange rules. Two mechanisms are responsible for the slight deviation from the collinear arrangement in the undoped and also in the doped  $\text{MgCu}_2\text{O}_3$ : the antisymmetric exchange interaction (Dzialoshinski-Moriya) and the differently oriented anisotropic  $g$  tensors of the spins in oppositely tilted  $\text{CuO}_6$  octahedra. Both mechanisms give rise to a canting angle in the same order of magnitude as the experimentally determined value. The effect of the differently oriented  $g$  tensors may be predominant in the case of  $\text{MgCu}_2\text{O}_3$ , because of the large tilting angle  $\alpha$  of the  $\text{CuO}_6$  octahedra.

The magnetic system can be separated into two magnetic subsystems, which are decoupled in the mean-field approximation. To understand the coupling mechanism between these subsystems one has to consider spin fluctuations, like thermal and quantum fluctuations and fluctuations of the local exchange field due to defects in the magnetic lattice. The thermal fluctuations (and the quantum fluctuations) stabilize a collinear arrangement between the spins of both subsystems. On the other hand, the fluctuations of the exchange field, e.g., caused by doping with nonmagnetic impurities, favor a strongly canted spin arrangement. The two magnetic phases in slightly Li-doped  $\text{MgCu}_2\text{O}_3$  demonstrate clearly, how these spin fluctuations and the fluctuations of the exchange field can determine the ground state of the whole system. The second magnetic phase transition in slightly doped

$\text{MgCu}_2\text{O}_3$  can be interpreted as a crossover from an almost collinear structure stabilized by thermal fluctuations at "high" temperatures to a strongly canted arrangement of the spins of the two subsystems below  $T_{N2}=35$  K. At low temperature the magnitude of the thermal fluctuations is lowered, thus the fluctuations of the exchange field due to the Li doping compensate the stabilizing effect for the collinear order and can induce the spin canting between the two sublattices.

It is remarkable, that a very low Li concentration of about 2 mole % —replacing approximately 0.5 at. % of the Cu atoms on the Cu site— is sufficient to destabilize the collinear order. The simple structural effect of substituting 0.5 at. % of the magnetic  $\text{Cu}^{2+}$  ions by  $\text{Li}^+$  is certainly not the main reason for the magnetic phase transition. A more effective disturbance of the magnetic lattice is the producing of electronic holes localized at the O atoms by  $\text{Li}^+$  doping. These localized electronic holes are also responsible for the observed variable-range-hopping conductivity.<sup>7</sup> The influence of localized and delocalized electronic holes on the magnetic state of the system  $\text{La}_{2-x}\text{Sr}_x\text{CuO}_4$  and  $\text{La}_2\text{Cu}_{1-x}\text{Li}_x\text{O}_4$  (Ref. 34) was theoretically discussed by Aharony *et al.*<sup>3</sup> As in the case of Li-doped  $\text{La}_2\text{CuO}_4$  the spins of the holes (i.e., of the  $\text{O}^-$  ions) in  $\text{Mg}_{1-x/2}\text{Li}_x\text{Cu}_{2-x/2}\text{O}_3$  should couple strongly ferromagnetically to the surrounding  $\text{Cu}^{2+}$  spins. This breaks up the antiferromagnetic order between the  $\text{Cu}^{2+}$  spins within the Cu-O chains. The magnetic frustration due to this effect is responsible for the drastic depression of the Néel state. In addition, the ferromagnetic clusters around the holes produce strong fluctuations of the local exchange fields at the positions of the surrounding Cu atoms. These ferromagnetic clusters and the diluting of the magnetic lattice combine to change drastically the ground state at low temperature to the strongly canted spin arrangement.

<sup>1</sup>J. G. Bednorz and K. A. Müller, *Z. Phys. B* **64**, 189 (1986).

<sup>2</sup>P. W. Anderson, *Science* **235**, 1196 (1987).

<sup>3</sup>A. Aharony, R. J. Birgeneau, A. Coniglio, M. A. Kastner, and H. E. Stanley, *Phys. Rev. Lett.* **60**, 1330 (1988).

<sup>4</sup>R. J. Birgeneau, M. A. Kastner, and A. Aharony, *Z. Phys. B* **71**, 57 (1988).

<sup>5</sup>H. Kamimura and A. Oshiyama, *Mechanisms of High- $T_c$  Superconductivity* (Springer-Verlag, Berlin, 1988).

<sup>6</sup>R. J. Birgeneau and G. Shirane, in *Physical Properties of High Temperature Superconductors I*, edited by D. M. Ginsberg (World Scientific, Singapore, 1989).

<sup>7</sup>M. Winkelmann, H. A. Graf, N. H. Andersen, T. Zeiske, and D. Hohlwein, *J. Magn. Magn. Mater.* **104-107**, 871 (1992).

<sup>8</sup>N. F. Mott and E. A. Davis, *Electronic Processes in Non-crystalline Materials* (Clarendon, Oxford, 1979).

<sup>9</sup>H. Drenkhahn and H. Müller-Buschbaum, *Z. Anorg. Allg. Chem.* **418**, 116 (1975).

<sup>10</sup>Th. Zeiske, H. A. Graf, and H. Dachs, *Solid State Commun.* **71**, 501 (1989).

<sup>11</sup>C. Friebel, V. Propach, and D. Reinen, *Z. Naturforsch.* **31b**, 1574 (1976).

<sup>12</sup>M. Winkelmann, H. A. Graf, B. Wagner, and A. W. Hewat, *Zeit. Kristallogr.* (to be published).

<sup>13</sup>J. B. Goodenough, *Magnetism and Chemical Bond* (Krieger, New York, 1976).

<sup>14</sup>J. Kanamori, *J. Phys. Chem. Solids* **10**, 87 (1959).

<sup>15</sup>B. Grande, H. Müller-Buschbaum, and M. Schweizer, *Z. Anorg. Allg. Chem.* **428**, 120 (1977).

<sup>16</sup>L. J. de Jongh, *Physica* **79B**, 568 (1975).

<sup>17</sup>K. B. Lyons, A. Fleury, J. P. Remeika, A. S. Cooper, and T. J. Negran, *Phys. Rev. B* **37**, 2353 (1988).

<sup>18</sup>J. C. Bonner and M. E. Fisher, *Phys. Rev.* **135**, A640 (1964).

<sup>19</sup>R. R. Gupta, in *Landolt-Börnstein, New Series II*, edited by O. Madelung (Springer-Verlag, Berlin, 1986), Vol. 16.

<sup>20</sup>N. W. Ashcroft and N. D. Mermin, *Solid State Physics* (Saunders College, Philadelphia, 1976).

<sup>21</sup>D. Reinen and C. Friebel, in *Structure and Bonding*, edited by J. D. Dunitz, J. B. Goodenough, P. Hemmerich, J. A. Ibers, C. K. Jørgensen, J. B. Neilands, D. Reinen, and R. J. P. Williams (Springer-Verlag, Berlin, 1979), Vol. 37.

<sup>22</sup>B. N. Figgis, *Introduction to Ligand Fields* (Interscience, London, 1966).

<sup>23</sup>P. J. Brown, in *International Tables for Crystallography* (Kluwer Academic, London, 1992), Vol. C.

<sup>24</sup>F. Keffer, in *Handbuch der Physik*, edited by S. Flügge (Springer-Verlag, Berlin, 1966), Vol. 18/2.

- <sup>25</sup>T. Moriya, Phys. Rev. Lett. **4**, 228 (1960); Phys. Rev. **120**, 91 (1960).
- <sup>26</sup>I. F. Silvera, J. H. M. Thornley, and M. Tinkham, Phys. Rev. **136**, A695 (1964).
- <sup>27</sup>L. J. de Jong, Solid State Commun. **65**, 963 (1988).
- <sup>28</sup>T. Ishikawa and T. Oguchi, Prog. Theor. Phys. **54**, 1282 (1974).
- <sup>29</sup>D. Welz, J. Phys. Condens. Matter **5**, 3643 (1993).
- <sup>30</sup>T. Oguchi, Phys. Rev. **133**, A1098 (1964).
- <sup>31</sup>J. Villain, R. Bidaux, J. P. Carton, and R. Conte, J. Phys. **41**, 1263 (1980).
- <sup>32</sup>E. F. Shender, Zh. Eksp. Teor. Fiz. **83**, 326 (1982) [Sov. Phys. JETP **56**, 178 (1982)].
- <sup>33</sup>C. L. Henley, J. Appl. Phys. **61**, 3962 (1987); Phys. Rev. Lett. **62**, 2056 (1989).
- <sup>34</sup>Y. Endoh *et al.*, Phys. Rev. B **37**, 7443 (1988).



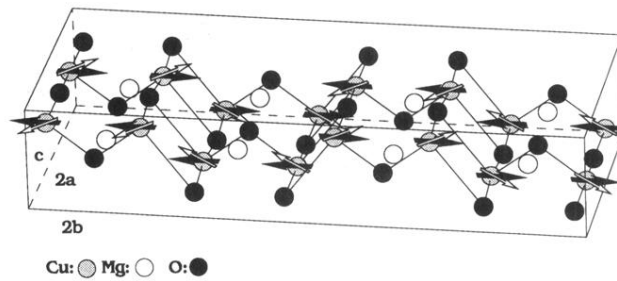


FIG. 1. The magnetic unit cell of  $\text{MgCu}_2\text{O}_3$ . The  $a$  and  $b$  axes are doubled as compared to the chemical unit cell. All spins in the upper part of the unit cell belong to the one magnetic sublattice, all spins in the lower part belong to the other sublattice. The spin arrangement for the undoped system is symbolized by the black arrows. In slightly Li-doped samples an additional phase transition occurs, where the spins of both sublattices are strongly rotated in opposite direction, giving rise to a large canting angle between the two sublattices. This is shown by the white arrows.

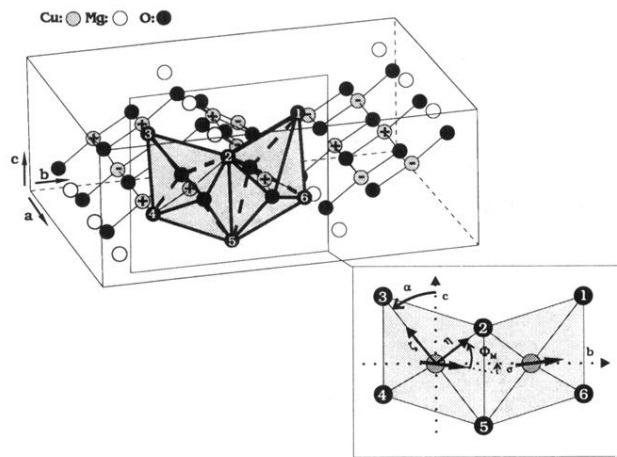


FIG. 2. The equatorial planes of the  $\text{CuO}_6$  octahedra are linked via common edges to form ribbons parallel to  $a$ . These ribbons are connected by approximately  $90^\circ$   $\text{O—Mg—O}$  and  $\text{Cu—O—Cu}$  bonds to a corrugated quasiplane. Adjacent  $\text{CuO}_6$  octahedra are tilted in opposite direction, giving rise to a weak spin canting in the undoped and doped system. This spin canting is shown in more detail in the inset.